# NUMERICAL EVALUATION OF THE MICRODAMAGE KINETICS OF CROSS-PLY GFRPS BASED ON STOCHASTIC MICRO-MESO MODELING

Sergei B. Sapozhnikov[1] and Alexandra A. Shabley[1]

[1]Aerospace Department, South Ural State University, Lenin ave., 76, Chelyabinsk, 454080, Russia
Email: sapozhnikovsb@susu.ru, Web Page: http://www.susu.ru

**Keywords:** stochastic fiber distribution, damage accumulation, matrix failure, FEA, modified CLT

**Abstract**
This paper presents an investigation of the effect of the random distribution of fibres on matrix cracks in [0m/90n/0m] glass fibre–epoxy laminates. Special C# software was developed to generate both the stochastic fibre distribution in 90° layers of different thickness in cross-ply laminates and text *.lgw file to run ANSYS FEA package. Using static loading, there were investigated stress-strain states of the matrix in 90° layers, distribution functions of fibre-to-fibre gaps and matrix cracks concentrations. Running of ANSYS (Autodyn3D, explicit formulation, ‘death of FE’ approach) allowed to get the matrix FE failure images, a stiffness reduction of 90° layers and to compare the results with non-FEA calculations using modified CLT - classical lamination theory - with CDM – continuum damage mechanics. There was proposed FARGR software for getting stress-strain curves until rupture of arbitrary laminates under monotonic increasing loads based on decreasing of layer’s stiffness due to longitudinal, transversal and shear mesodamages accumulation.
The general purpose of the paper is to estimate the possibility of substitution of time-consuming explicit FEA investigations of nonlinear mechanical behaviours of FRPs by the fast and effective FARGR-calculations.

## 1. Introduction

Composite materials are widely used in modern industry (aircraft and automotive, construction, etc.). It should be noted that modern high-strength and lightweight composite materials (glass, carbon or aramid FRPs) are significantly more expensive than steel and aluminium alloys, exhibit the properties of elastic and strength anisotropy, have a nonlinear deformation because of microdamage progression and are relatively small (in comparison with metals) deformation of failure.
Damage in FRPs develops in stages and is connected to the material’s microstructure at different scales [1]. In cross-ply laminates subjected to tension, the damage starts in transverse (90) layers preferably as matrix failure. Stress concentrations into fibre-to fibre gaps drive the matrix failure due to the mismatch in transverse stiffness of the fibre and the matrix. Microscale damage in the matrix develops into transverse ‘cracks’ until the cracking process saturates, depending on matrix properties and internal fibre stacking geometry [2-6]. Eventually, transverse cracks contact adjacent longitudinal plies and may start interlaminar delaminations. The damages lead down to the load-carrying capacity of the material commonly observed as a reduction of stiffness [6]. The process of damage nucleation and development is very well understood for both composite cross-ply laminates and composites with plain textile reinforcement [7]. The idea of layer stiffness reduction is the base of popular approach named Continuum Damage Mechanics (CDM) [8, 9]. This approach correctly reflects the effect of damages accumulation on the overall mechanical performance of composites in WWFE I and III [10, 11]. CDM in its classical formulation is also not able to reproduce interactions between different damage types, such as intraply matrix cracks and delaminations. One such approach based on non-local

CDM for intraply cracks and cohesive zone method (CZM) for delaminations was applied to modelling of damage in laminates [12]. Difficulties in the implementation of CZM has led to the development of other methodologies [12-14].

The present work concentrates on assessing the performance of explicit FEM in ANSYS Autodyn® for modelling of progressive microdamages in a matrix between fibres into 90° layers of cross-ply GFRP and simplified scheme with a substitution of micromodel of GFRP by modified CLT with cumulative mesodamage mechanics to predict nonlinear stress-strain curve by using developed easy-to-use FARGR software.

## 2.Micro modelling

There was developed special C# software (with the convenient graphical user interface, Fig.1) to generate *Result.lgw* text file of the stochastic fibres distribution in the rectangular area. This area (as 90° layer in cross-ply laminate) has known length a, thickness c and b of 0° and 90° layers and diameter df of fibres (with possible variation). There are required fibre volume fraction *V* and minimal value δ of fibre-to-fibre and fibre-to-adjacent 0° layers gap (this is needed to further use ANSYS® modelling to prevent the presence of extremely small finite element size). The brief description of the algorithm of a stochastic fibres distribution generation is as follows. For required volume fraction there was calculated the total number of fibres $N_f$ to put into the a*b area. Then each *i*-fibre ($i=1 \ldots N_f$) was 'dropped down' into this rectangular area by using stochastically generated $x_i$ and $y_i$ co-ordinates. The program checked the overlapping of fibres, intersecting with borders of the area, eliminated overlapped fibres and made next attempt to drop down new fibre into the free space. Each step is finalised by calculation of real fibre volume fraction and compared with required value *V*. If the discrepancy was less than 1% calculation procedure stops. Fig.1 illustrates the stochastic fibres distribution for given *a, b, c*, $d_f$ and $\delta$ for *V*=0.5 and the *Result.lgw* file.

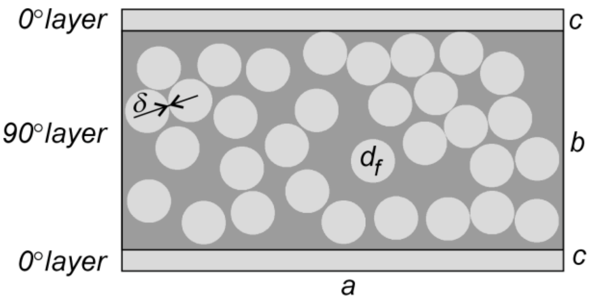


```
/PREP7
BLC4,0,0,2.000e-002,1.000e-003,1.000e-003
BLC4,0,1.000e-003,2.000e-002,1.000e-002,1.000e-003
BLC4,0,1.100e-002,2.000e-002,1.000e-003,1.000e-003
CYL4,2.525e-003,6.355e-003,1.000e-003, , , ,1.000e-003
CYL4,1.759e-002,4.992e-003,1.000e-003, , , ,1.000e-003
…
CYL4,1.156e-003,4.674e-003,1.000e-003, , , ,1.000e-003
CYL4,1.119e-002,2.486e-003,1.000e-003, , , ,1.000e-003
CYL4,1.559e-002,5.366e-003,1.000e-003, , , ,1.000e-003
vovlap, all
vglue, all
```

**Figure 1.** The image and shortened *Result.lgw* data file of stochastic fibres distribution (real V=0.503).

It is known that fibre-to-fibre gaps play the general role to stress concentration and failure of the matrix into 90 layers [15, 16]. The result of stochastic fibre stacking shown on the Fig.2 as the exponential cumulative function *1-exp(-kx)* where *x* – relative gap $\delta/d_f$ and *k*- empirical constant equal 3.90.

Using ANSYS Autodyn® FEA software (explicit formulation, mass scaling for quasi-static loading conditions), we investigated the stress-state and damage accumulation (plane strain, Fig.3) of the matrix under tension of cross-ply glass-epoxy resin laminate [0/90$_5$/0] with the length of 50 mm. Having $\delta=d_f/100$ and *V*=0.5 Fig.3 illustrates the matrix cracks' progression. Here we use the mean first principal stresses in the matrix as the left part of the failure condition $\sigma_1 \geq F$ to 'kill' FE (*F*=100 MPa).

Mechanical characteristics of the model parts shown in Tab.1. Here *E* – modulus of elasticity, $\nu$ – Poisson ratio, *F* – tensile strength of matrix, * denotes $E_1$ and $\nu_1$ for UD GFRP.

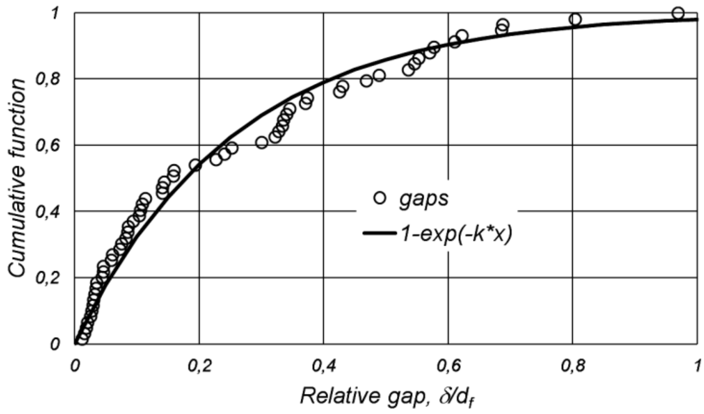


**Figure 2.** Fibre-to-fibre gap's distribution ($k$=3.90).

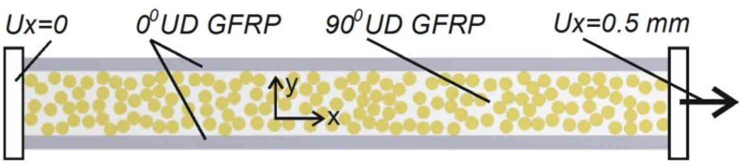


**Figure 3.** Testing sample of $[0/90_5/0]$ GFRP.

**Table 1.** Mechanical behaviours of constituents.

| Material | $E$ (GPa) | $v$ (GPa) | $F$ (MPa) |
|---|---|---|---|
| Glass fibre | 73 | 0.25 | - |
| Epoxy matrix | 3.78 | 0.35 | 100 |
| 0° UD layer | 40* | 0.30* | - |

During numerical 'testing' of $[0/90_5/0]$ sample we can observe the 'load – displacement' curve, Fig.4, black line.

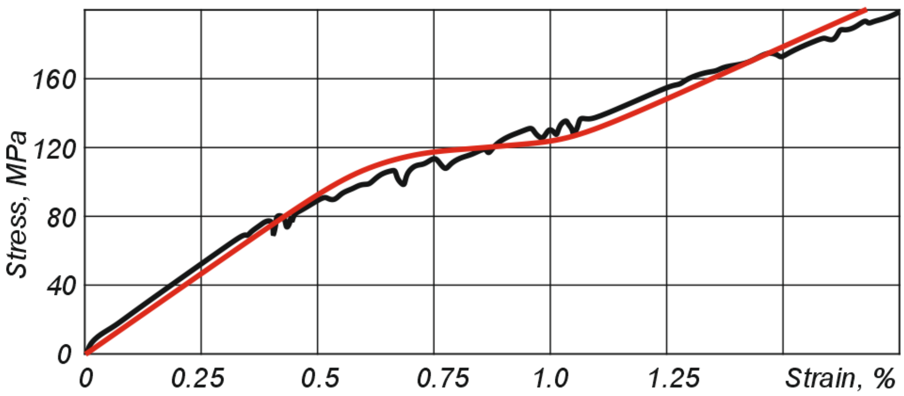


**Figure 4**. Load – displacement curves of tested sample. Black line – FEA calculation, red line – FARGR calculation (chapter 3).

Looking at this figure, we can see several big amplitude oscillations connected with through-thickness cracks' formation and multiple smaller amplitude ones generated by local microdamages. Having longer model, we will get a smoother load-displacement curve.
The microdamage development can be seen on Fig.4. Here are through-thickness 'cracks' and multiple smaller and complex shaped damages, so it's hard to calculate the exact final crack density – the very popular parameter of theories operated with it [12-16].

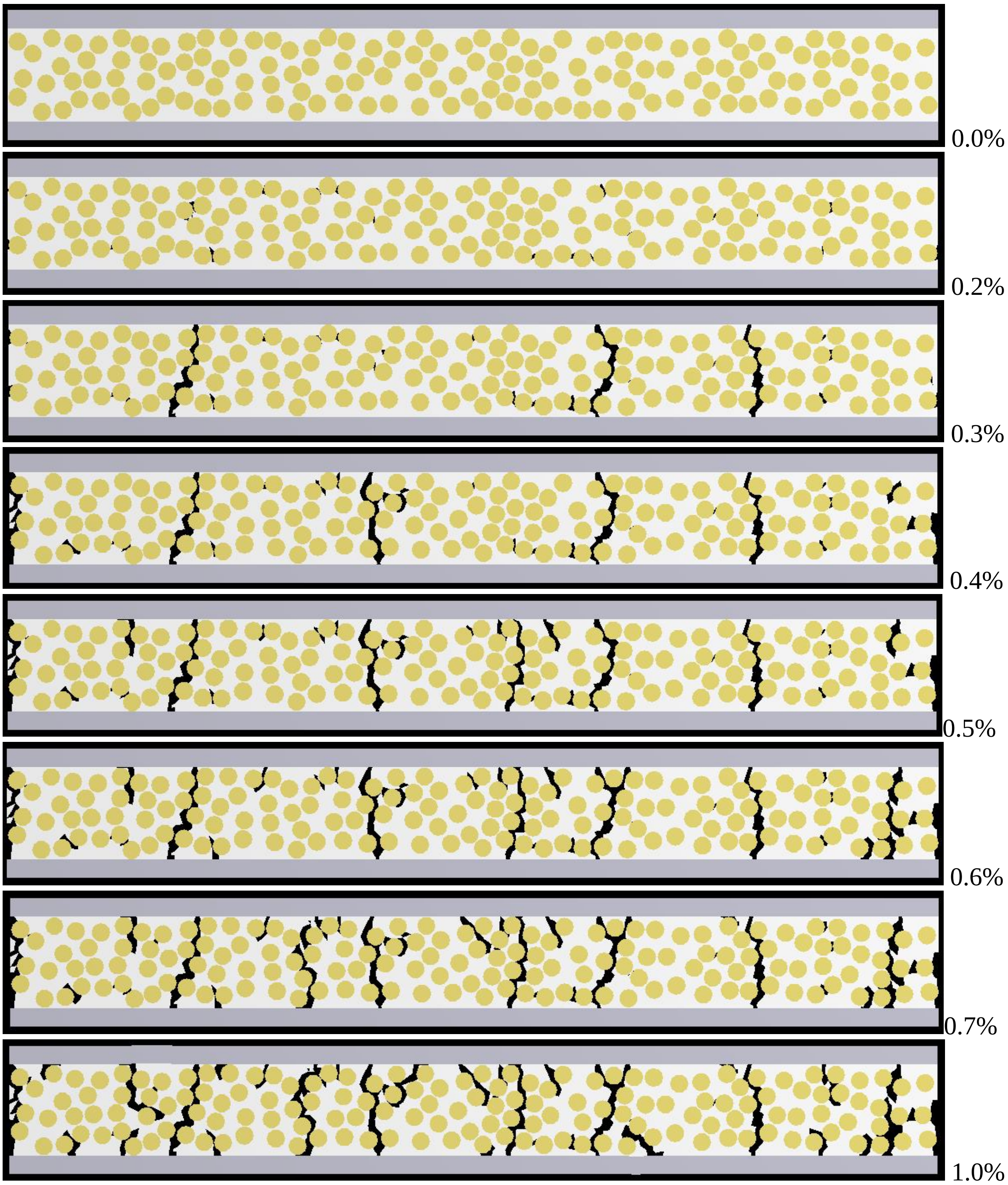


**Figure 5**. Microdamage development with tension strain increasing (on the right).

## 3. FARGR software

Direct calculations of ‘load - displacement’ curve of cross-ply laminate required explicit CPU-expensive numerical procedures connected with FE methodology. It is impossible to use the very long testing sample (to get smooth ‘load - displacement’ curve) because of a time-consuming deal. So, that is reasonable to substitute real-time calculation by quasistatic semianalytical one with taking into account of CDM – continuum damage mechanics together with CLT and decreasing of layer stiffness by mesodamage accumulation [10]. Modified CLT operates with an absolutely stable procedure of solving the linear system of equation with variable ply elastic behaviours (secant moduli).

In this technology the ply mesodamages are possible in fibre (longitudinal), matrix (transverse) and shear directions – $\omega_1$, $\omega_2$ and $\omega_3$ ($0 \leq \omega \leq 1$). These mesodamages are independent (to simplify calculations) to take into account only connections with separately ply stresses along fibres $\sigma_1$, across $\sigma_2$ and shear $\tau_{12}$. Secant (superscript ‘s’) moduli of ply are the functions of only $\omega_1$, $\omega_2$ and $\omega_3$:

$$E_1^s = E_1 * (1-\omega_1),\ \nu_1^s = \nu_1 * (1-\omega_1),$$
$$E_2^s = E_2 * (1-\omega_2),\ G_{12}^s = G_{12} * (1-\omega_3). \qquad (1)$$

Here $E_1$, $E_2$, $G_{12}$ and $\nu_1$ – initial moduli of ply. For getting $\omega_i(\sigma_i)$,where $i=1,2$ and $3$, it is needed to have the strength of ply in longitudinal, transversal and shear directions (can be found in reference books). Moreover, it needs to have the standard deviations of fibre strength, matrix strength and shear strength of local volumes of UD composite (for each ply in laminate composite). Understanding the difficulties of getting this statistical info we offered to take into account Gaussian (normal) distribution of the local strength of constituents and the variational coefficient equal 0.2 for all these directions. All assumptions are listed in [11] (using popular PTC MathCAD shell) and well confirmed by comparison with the experimental data of WWFE [10].

In this work we proposed to use FARGR as stand-alone software (free of charge after the request on the email) having the convenient graphic user interface, Fig.4.

The left column is the place to input elastic, strength and loading data together with ply stacking sequence information. ‘Calculation’ button being pressed once starts the program and shows the results in a second in the main graphical area.

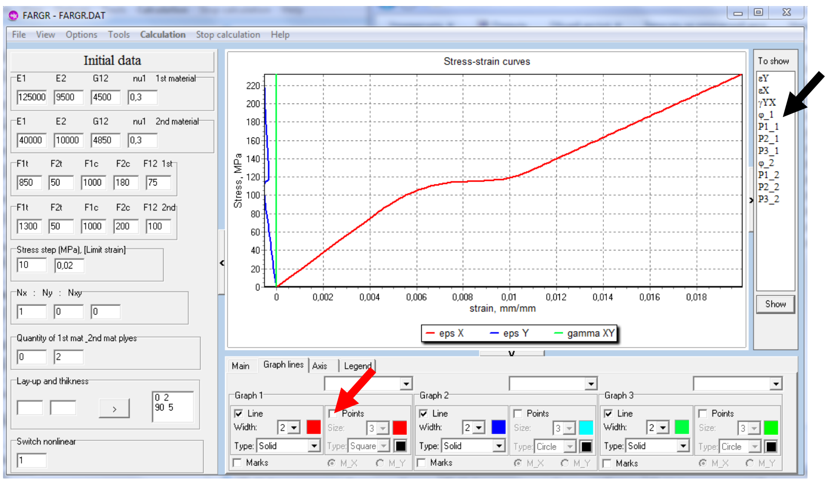


**Figure4.** Graphic user interface of FARGR software.

Input data here are those to calculate strains on given stresses of the red line on the Fig.4. By the way, using the column on the right window (black arrow, Fig.4) it is possible to see stacking angle variation

– so-called ‘scissoring’ effect during tension of angle-ply laminates (φ_1, φ_2 etc.), damages progression of first ply (P1_1, P2_1, P3_1), second ply (P1_2, P2_2, P3_2), etc. Changing the graphical style of curves we can see the pure elastic initial part of the stress-strain diagram (rarely marked) and non-linear part (densely marked) connected with mesodamage initiation and accumulation, selecting option ‘Points’ on the bottom window (red arrow, Fig.4 and black arrows, Fig.5).

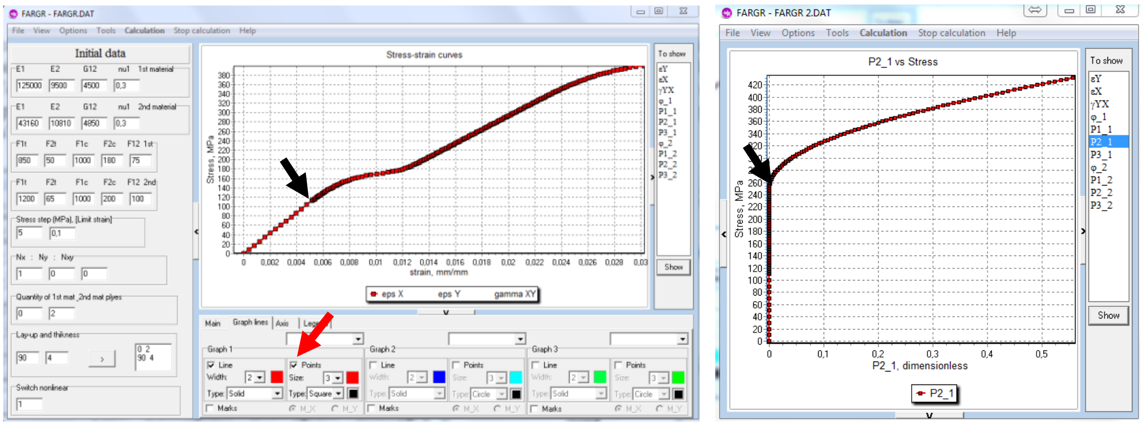


a b

**Figure 5.** Optional marked stress-strain curve (a) and mezodamage P2-1 ($\omega_2$) progression (b).

To have additional confirmation of the stress-strain prediction quality by FARGR the comparison of experimental curves [17] for cross-ply laminates with predicted ones shown on Fig.5. For this case elastic moduli [17] $E_1$ = 43.16 GPa, $E_2$ = 10.81 GPa, $G_{12}$ =4.85 GPa, $\nu_1$ =0.306, and strength data (estimated values) $F_{1t}$ =1200 MPa, $F_{2t}$ =65 MPa.

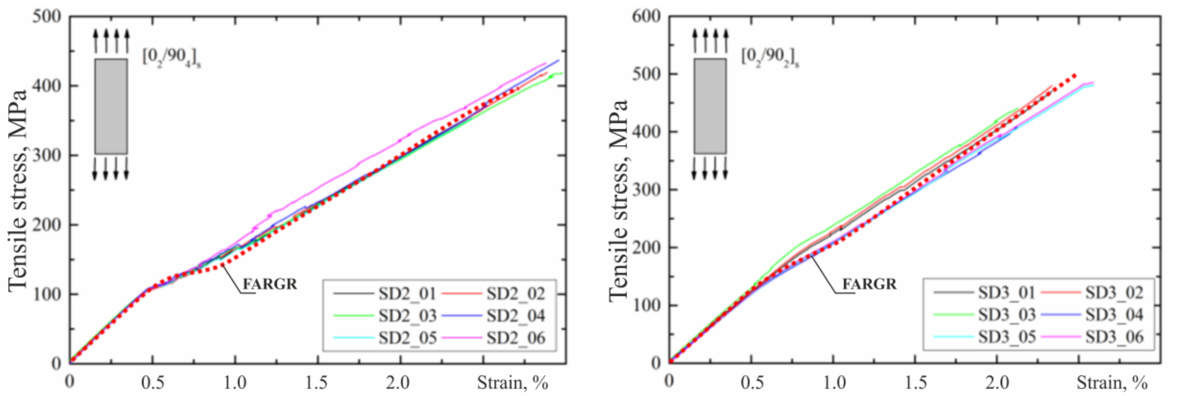


**Figure 5.** Experimental [17] and semianalytical (red dotted lines, FARGR) stress-strain curves of $[0_2/90_4]_s$ and $[0_2/90_2]_s$ GFRPs.

Moreover, authors of [17] published the observations of the applied stress for *initiation of cracking* in 90° and 0° plies for investigated samples of cross-ply GFRPs. We have made the comparison of these stresses with predicted (**bold**) ones using FARGR, Table 2.

**Table 2.** The details of cracking in composites.

| Lay-up | $[0_2/90_2]_s$ | Error | $[0_2/90_4]_s$ | Error |
|---|---|---|---|---|
| Applied stress for transverse crack initiation (90° ply), MPa | 185/**140** | -24% | 105/**110** | +5% |
| Applied stress for longitudinal crack initiation (0° ply), MPa | 423/**450** | +4% | 255/**275** | +8% |
| Maximum failure stress, MPa | 490/**590** | +20% | 430/**390** | -9% |

The average error of the crack initiation stress is ~10%. The average error of the strength prediction is ~15%. For the engineering applications, this quality of the strength and the crack initiation stress predictions are quite well.

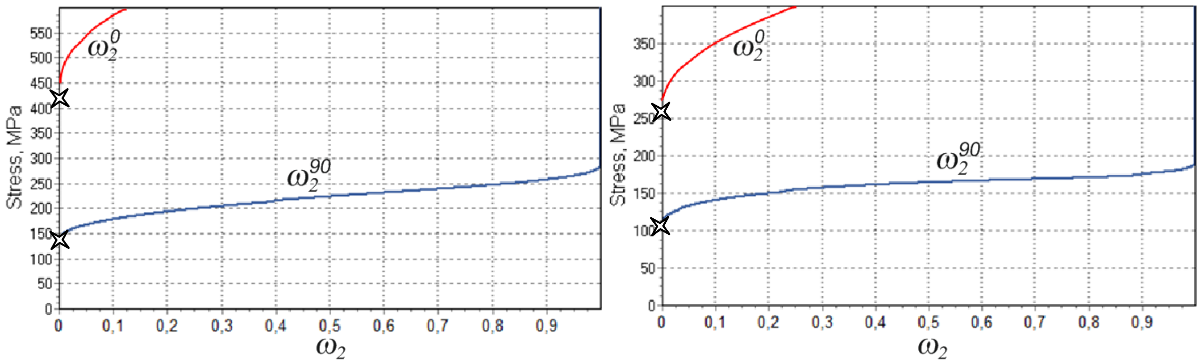


a b

**Figure 6.** Stresses of the crack initiation and progression of mesodamages: (a) $[0_2/90_4]_S$, (b) $[0_2/90_2]_S$. Asterisk denotes the experimental stress of cracks initiation.

## 4. Conclusions

The microdamage development in 90 plies of the cross-ply laminate shown that only in the early stages there is so-called 'crack density' which can be exactly calculated. But with increasing of longitudinal strain the pictures of damaging become more complicated, there are numbers of small cracks reduced the stiffness of 90 plies until saturation. This fact led to the possibility to substitute time-consuming explicit FEA with the discrete development of damage process on a smooth cumulative damage mechanics into Classical Lamination Theory (semianalytical and fast FARGR software). Numerical, experimental and semianalytical results are in good correlation.
FARGR software can predict the stress-strain curves for composites constructed with any stacking sequence of one or two different UD plies (CFRP, GFRP or AFRP). So, it is possible to predict the mechanical nonlinearity of such hybrids with alternating layers.
Very simple basics of FARGR led to use this software only as the first iteration. The second one should be the experiment or more detailed numerical 'test'.

## Acknowledgments

This work was financially supported by the Russian Science Foundation (project No. 18-19-00377). The authors also gratefully acknowledge L.Shipulin and A.Ignatova for the help in C# programming.

**References**

[1] L. Gorbatikh, S.V. Lomov. Damage in architectured composites. Comprehensive Composite Materials II, *Volume 2: Polymer Matrix Composites: Fundamentals*, Elsevier Science & Technology Books; 2017.

[2] J.A. Nairn. Matrix Microcracking in Composites. In: Zweben A.K., editor. *Comprehensive Composite Materials. Oxford: Pergamon,* 2000. p. 403-32.

[3] S.G. Ivanov, D. Beyens, L. Gorbatikh L, S.V. Lomov. Damage development in woven carbon fibre thermoplastic laminates with PPS and PEEK matrices: A comparative study. *Journal of Composite Materials,* 51:637-647, 2017.

[4] M.G. Callens, L. Gorbatikh, I. Verpoest. Ductile steel fibre composites with brittle and ductile matrices. *Composites Part A - Applied Science and Manufacturing,* 61:235-44, 2014.

[5] M.G. Callens, L. Gorbatikh, E. Bertels, B. Goderis, M. Smet, I. Verpoest. Tensile behaviour of stainless steel fibre/epoxy composites with modified adhesion. *Composites Part A - Applied Science and Manufacturing,* 69:208-18, 2015.

[6] S.L. Ogin, P .Brøndsted, J. Zangenberg. Composite materials: constituents, architecture, and generic damage. *Modeling Damage, Fatigue and Failure of Composite Materials,* Woodhead Publishing; p. 3-23, 2016.

[7] L. Gorbatikh, S.V. Lomov. Damage accumulation in textile composites. *Modeling Damage, Fatigue and Failure of Composite Materials,* Woodhead Publishing, p.41-59, 2016.

[8] P. Maimi, P.P. Camanho, J.A. Mayugo, C.G. Davila. A continuum damage model for composite laminates: Part I - Constitutive model. *Mechanics of Materials,* 39:897-908, 2007.

[9] P. Maimi, P.P. Camanho, J.A. Mayugo, C.G. Davila. A continuum damage model for composite laminates: Part II - Computational implementation and validation. *Mechanics of Materials.* 39:90–99, 2007.

[10] S.B. Sapozhnikov, S.I. Cheremnykh, A.S. Maslakova. Prediction of deformation and biaxial strength of fiber reinforced laminates for WWFE by using micro damage mechanics. *Proc. of 13th European Conference of Composite Materials (ECCM-13), Stockholm Sweden*, June 2-5, 2008.

[11] S.B. Sapozhnikov, S.I. Cheremnykh. The strength of fibre reinforced polymer under a complex loading. *Journal of Composite Materials*, 47:20-21, 2525-2552, 2013.

[12] F.P. Van der Meer, C.G. Davila. Cohesive modeling of transverse cracking in laminates under in-plane loading with a single layer of elements per ply. *International Journal of Solids and Structures,* 50:3308-18, 2013.

[13] A. Hansbo, P. Hansbo. A finite element method for the simulation of strong and weak discontinuities in solid mechanics. *Computer Methods in Applied Mechanics and Engineering,* 193:3523-40, 2004.

[14] J.M. Berthelot, J.F. Le Corre. Statistical analysis of the progression of transverse cracking and delamination in cross-ply laminates. *Composites Science and Technology,* 60:2659-69, 2000.

[15] P. Lundmark, J.Varna. Constitutive relationships for laminates with ply cracks in in-plane loading. *International Journal of Damage Mechanics*, 14: 235–261, 2005.

[16] E.J. Barbero, D.H. Cortes. A mechanistic model for transverse damage initiation, evolution, and stiffness reduction in laminated composites. *Composites Part B: Engineering,* 41(2):124-132, 2010.

[17] H. Shen, W. Yao, W. Qi, J. Zong. Experimental investigation on damage evolution in cross-ply laminates subjected to quasi-static and fatigue loading. *Composites Part B: Engineering*, 120:10-26, 2017.